A NOVEL PROTECTION SCHEME FOR INVERTER-DOMINATED MICROGRID

Di Liu [1*], Dimitrios Tzelepis[1], Adam Dyśko[1], Campbell Booth[1]

[1]Department of Electronic and Electrical Engineering, University of Strathclyde, Glasgow, United Kingdom
**d.liu@strath.ac.uk*

Keywords: MICROGRID PROTECTION, INVERTER DOMINATED MICROGRID, DISCRETE WAVELET TRANSFORM, HIGH IMPEDANCE FAULT

Abstract

Protecting an inverter-dominated microgrid is challenging for the traditional overcurrent protection scheme owing to the suppressed fault current from the inverter interfaced DGs (IIDGs). In this paper, a protection scheme based on the Discrete Wavelet Transform is developed in MATLAB/SIMULINK to detect the faults in the microgrid. The input voltage of the proposed scheme is first transformed into dq0 frame using the Park Transform. A filtering system based on the wavelet denoising approach is then implemented to reduce the sampling frequency and reject the switching noise generated by the inverters in the microgrid. The performance of the proposed scheme is evaluated in transient simulation by systematically applying different types of faults, including varied fault positions and impedances. Additionally, a high impedance arcing fault model is implemented to test the proposed protection scheme under nonlinear fault impedance conditions.

1 Introduction

In recent years, driven by the energy depletion and the climate change, the number of distributed generators (DGs) powered by renewables has increased significantly in many countries [1]. However, some technical constrains related to voltage stability, power flow and protection, can seriously limit further penetration of these renewables in the future [2][3].

Microgrid is a small-scale network comprising the distributed generators, loads and storage, which provides an effective solution for the accommodation of renewables. In normal condition, the microgrid delivers its surplus generation to the main network as an equivalent current source. When a fault occurs in the distribution network, the microgrid is disconnected and operates independently as an 'islanded microgrid'. The protection issues of the microgrid are mainly related to the islanded operation due to the suppressed fault level especially when the microgrid is dominated by the inverter-interfaced DGs. The fault current from these generators is usually limited to 2 p.u [4], which cannot be reliably protected using the traditional overcurrent relays. Additionally, considering the low inertia of the inverter-dominated microgrid, the protection scheme must be fast enough to isolate the fault or the electronic devices in the microgrid or else the stability of microgrid could be compromised.

As a crucial part during the implementation of microgrid, some protection schemes have been proposed in technical literature. As a typical example, adaptive protection schemes are proposed in [5]-[7]. In the adaptive protection schemes, the relay setting can be attuned, based on the prevailing system status which is captured using a monitoring system such as SCADA. Therefore, an advanced communication system is usually required in most adaptive protection schemes which increases the practical implementation cost. Additionally, the information cybersecurity needs to be carefully considered in the future applications. Differential based protection schemes are used in [8] for the protection of the medium-voltage microgrid. Based on the validated results, the relay can clear the faults quickly, and as demonstrated in the paper, the proposed protection scheme is still valid during the high impedance fault conditions. However, as the involvement of communication channels and the GPS measuring system, the price of this protection scheme is quite expensive. Travelling wave based system is employed for the protection of a 20 kV microgrid in [9]. The polarity of the travelling wave is processed by using the mathematical morphology (MM) method and used as the tripping criteria of this protection scheme. Although it has a good performance in various scenarios, the high sampling frequency is compulsory in this method. Therefore, it is not suitable for the protection of the low voltage microgrid (400 V) with the short-length feeders. Some other protection schemes for the microgrid can be found in [10].

When fault occurs in the microgrid, a transient signal is created in the voltage and current, which provide a good fault indicator. However, in some situations such as the high impedance fault scenario, these transients are not obvious and may be hard to capture by conventional relays. Therefore, an advanced signal processing method is needed to extract the fault information from the transient signal. In this paper, a Discrete Wavelet Transform (DWT) tool is utilized. Additionally, to reduce the requirements for very high sampling frequency, and at the same time, reject the noise from the fast switching of the inverters, an effective denoising system is developed using the

wavelet denoising approach. This paper is organized as follows. Section 2 describes the algorithm of the protection scheme. Section 3 discusses the test microgrid model used to evaluate the performance of the proposed scheme. The simulation results and the conclusions are presented in sections 4 and 5 respectively.

2 DWT based Protection Scheme

2.1 System Overview

The proposed protection scheme utilises the measured terminal voltage of the inverter in the microgrid. The entire scheme is divided into three stages as displayed as Fig. 1. The operating principles of the scheme are explained in detail in the following sections.

2.2 Stage 1 : Park Transform and Wavelet Denoising

Park Transform implemented is used to transform the measured voltage in natural abc phase frame into dq0 frame. In balanced steady state condition, the voltage on dq0 frame is a pure DC component, but if a fault occurs in the system, the AC ripple is added on the transformed voltage [11]. This characteristic can be utilised conveniently for fault detection. Moreover, the park transform aided DWT decreases the memory space requirements and computational burden on the numerical relays [12].

In the inverter dominated microgrid, the noise will be created by the fast switching of inverters. Although some of this noise can be removed using the filter designed by the inductor and capacitor such as LC and LCL filter, there still exists some noise level in the signal, which degrades the performance of the protection system particularly in the case of high impedance fault. A wavelet based denoising system is developed to address the noise issue in the microgrid. Firstly, the DWT divides the input signal into different frequency bands, which allows to present the signal using the coefficients at different wavelet levels. Comparing with useful signal, the coefficients of noise are relatively small, therefore, the signal disturbance can be filtered through replacing the coefficients under the defined threshold by zero. 'Haar' wavelet is employed for design of the filter and the threshold is established using the soft threshold approach given by the following equation where Δx is the threshold of the filter and x is the wavelet coefficients at a given level.

$$y = \begin{cases} sign\,(|x| - \Delta x), |x| > \Delta x \\ 0, \quad |x| \leq \Delta x \end{cases} \tag{1}$$

2.3 Stage 2 : Tripping Variables Definition

The wavelet coefficients of the denoised signal are computed using the db4 wavelet. The energy feature of the coefficients is calculated by the following equation (2) [13].

$$E_i = \sum_{j=1}^{n_i} |d_{ij}|^2 \tag{2}$$

where i=1,2….,I stand for the scale, and j=1,…n_i stand for the number of the used coefficients in each calculation cycle. In this scheme, the sampling period for energy calculation is 0.02 s, and the sampling frequency is 1 kHz, which means the new energy value is evaluated every 20 samples.

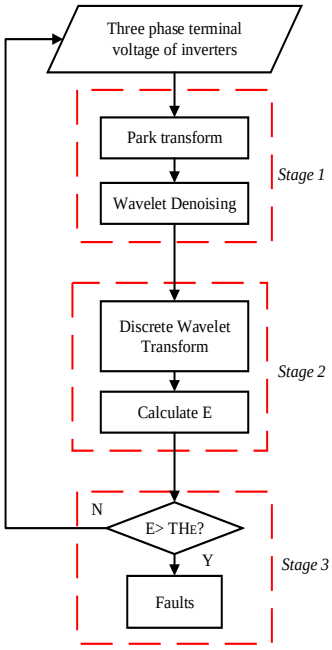

Fig. 1 Algorithm of the proposed protection scheme.

2.4 Stage 3 : Tripping Threshold Decision

The choice of tripping thresholds, TH_E, has a significant influence on the performance of the proposed scheme. With the help of the wavelet denoising system, the magnitude of the noise energy can be limited to 20. Moreover, a 50% safety margin has been considered during the threshold setting process owing to the stability requirement. At the end, the tripping threshold is set as $TH_E = 30$.

3 Studied Microgrid System

In this paper, a 400 V, 50 Hz, a model of the benchmark microgrid [14] is developed in MATLAB/SIMULINK environment to evaluate the performance of the proposed protection scheme.

The single line diagram of the test microgrid is shown in Fig. 2, where 'L1, L2,...' stand for the feeders connecting two nodes. The detailed parameters of the feeders are included in [14]. There are four inverter interfaced DGs in this microgrid. DG1 is the master unit, which is responsible for providing the voltage and frequency reference to the islanded microgrid and the other three DGs are the slave units, which deliver constant power to the grid. Moreover, owing to the safety requirement of the inverters, the fault current of each inverter interfaced DG has been limited to 1.2 times of the rated current [15]. In this microgrid, the total capacity of the generators is 60 kW and the rated power of every load is 10 kW. The switch at the top of this diagram is used to change the structure of this microgrid, i.e. normally open point.

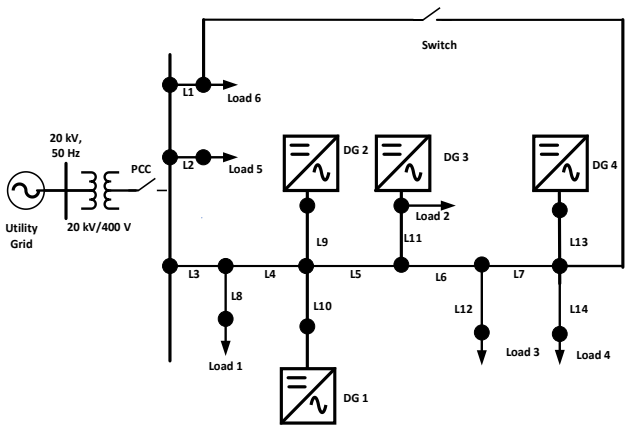

Fig. 2 Low-voltage benchmark microgrid.

4 Simulation Results and Analysis

In this section, several case studies are presented to demonstrate the performance of the proposed scheme in the islanded microgrid. The input voltage of the protection scheme is measured at the terminal of DG3 and the sampling frequency is 1 kHz. In the following parts, the symbol *E* stands for the energy of wavelet coefficients and the logic value '1' of the trip signal means the fault has been detected by the relay. The test scenarios are listed in Table 1 , where 'SPG', 'PPG' and 'PPPG' stand for the single phase to ground, phase to phase to ground and three phase to ground fault respectively. These faults occur at the medium point of each feeder at 0.3s. Furthermore, the fault scenarios will be implemented in the radial and looped microgrid to evaluate the performance of the scheme under different microgrid structures.

Table 1 Fault scenarios in the test.

Case Number	Fault Type	Fault Resistance	Fault Position
Case 1	SPG	0.1 Ω	L5
Case 2	SPG	100 Ω	L5
Case 3	PPG	0.1 Ω	L6
Case 4	PPPG	0.1 Ω	L7

4.1 Case 1: Single phase to ground fault in L5 (LIF)

In this case study, a single phase to ground fault with 0.1 Ω impedance has been applied at the middle point of Line 5 to evaluate the performance of the proposed scheme in the case of low impedance fault (LIF). The results for the radial and looped microgrid are shown in Fig. 3 and Fig. 4 respectively, where the maximum values of *E* have been limited to 100 to enable clearer observation. From these figures, the magnitude of the pre-fault noise energy has been suppressed to lower than 20 successfully by using the denoising system. When the fault occurs, the value of *E* increases sharply and reaches the threshold '$TH_E = 30$ (the dashed red line)' rapidly, and the relay detects the fault within 50 ms.

4.2 Case 2: Single phase to ground fault in L5 (HIF)

In this case, the scheme performance is tested under the high impedance fault (100 Ω) scenario. Considering the non-linear nature of the high impedance fault (HIF), the fault model included in [16] is employed in this paper as shown in Fig. 5, where two DC sources, V_p and V_n and two resistances, R_p and R_n, represent the arcing voltage and fault resistances of air in soil or between trees and distribution feeders respectively [17]. The values of V_p and V_n are determined by the physical features of the contacting material. For example, the density and the amount of moisture of sandy soil have a major influence on the choice of V_p and V_n [16]. In this case study, the values of V_p and V_n set as 200 V and the values of R_p and R_n set as 95 Ω and 105 Ω, varying in the range of $\pm 5\%$ around the assigned (mean) value, to mimic the asymmetrical feature of the high impedance fault [18]. The result in the radial microgrid is shown in Fig. 6. Comparing with the result of case 1, the maximum value of the energy has decreased owing to the increase of the fault impedance, and the wavelet energy oscillates between 30 and 100, but the scheme can still detect the fault in less than 70 ms, which is fast enough for low voltage (400 V) network applications. The similar result can be achieved when the structure of the microgrid changes to the loop as shown in Fig. 7. Overall, it can be concluded that the performance of the proposed system is not influenced by the variation of the microgrid structure.

4.3 Case 3: Phase to phase to ground fault in L6

In this case study, a phase to phase to ground fault has been added at the midpoint of line 6. Comparing with the result of case 1, the faults in case 3 have been detected faster as shown in Fig. 8 and Fig. 9, as the oscillated voltage in the d axis has a higher magnitude than the values in the single line to ground fault. Based on results in Fig. 8 and Fig. 9, the proposed protection scheme can detect the fault in less than 40 ms, and it is immune to the change of the microgrid structure.

4.4 Case 4: Three phase to ground fault in L7

Comparing with asymmetrical faults, the balanced fault is harder to be sensed by the relays owing to the loss of the information about the negative and zero sequence components. When the three phase to ground fault occurs in the microgrid, the voltage in the d axis is still a DC component, which is the same as the normal condition. However, a falling edge will be introduced owing to the voltage drop during the fault period. This can be detected by the DWT based protection scheme as shown in Fig. 10 and Fig. 11. Based on the simulation results, the balanced faults can be detected by the relay within 40 ms. Additionally, the detection of three phase to ground fault is not influenced by the microgrid structure.

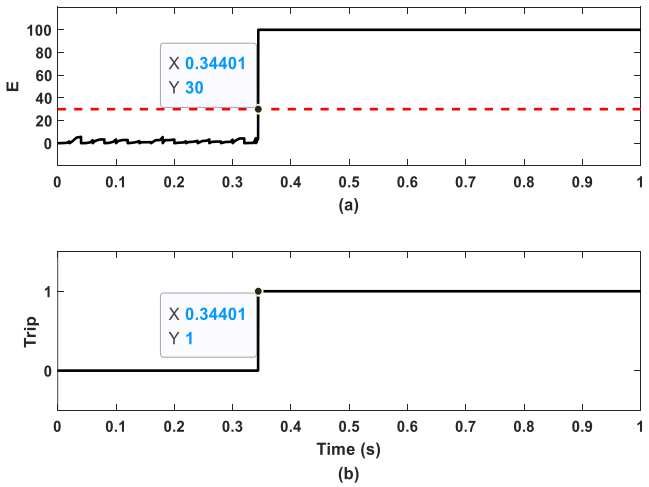

Fig. 3 Low impedance fault in radial microgrid.
(a)Wavelet energy.
(b)Trip signal.

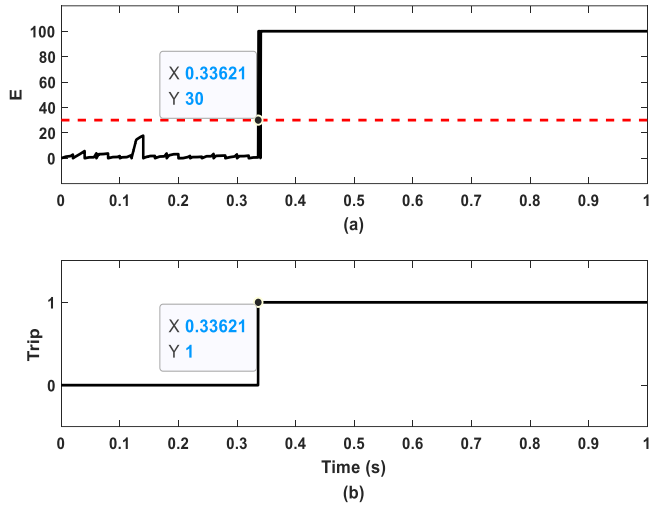

Fig. 4 Low impedance fault in looped microgrid.
(a)Wavelet energy.
(b)Trip signal.

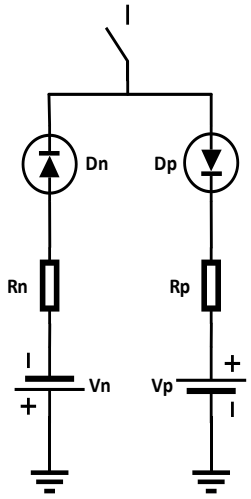

Fig. 5 High impedance fault model used in the test.

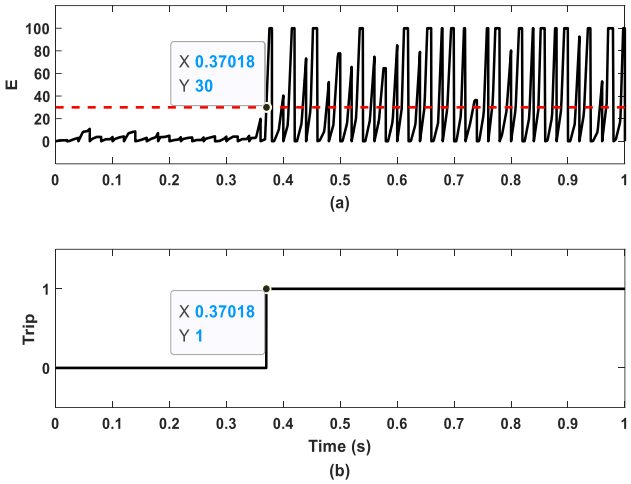

Fig. 6 High impedance fault in radial microgrid.
(a)Wavelet energy.
(b)Trip signal.

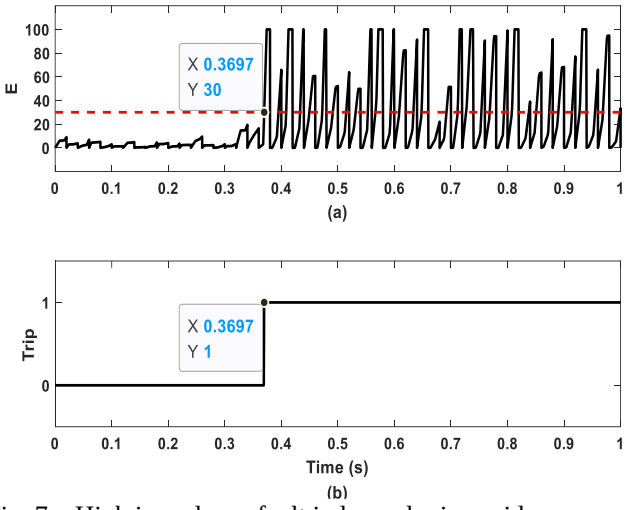

Fig. 7 High impedance fault in looped microgrid.
(a)Wavelet energy.
(b)Trip signal.

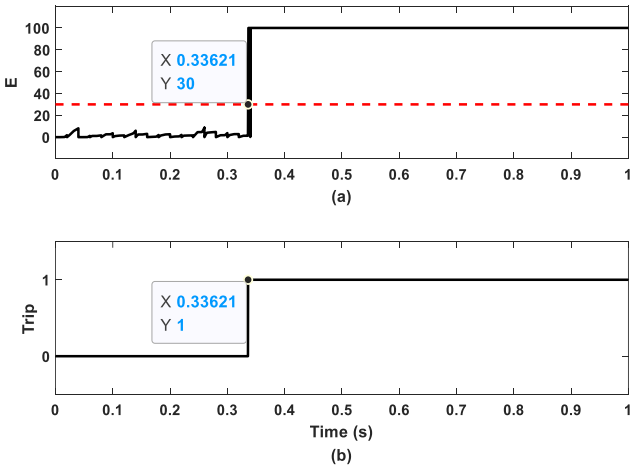

Fig. 8 Phase to phase to ground fault in radial microgrid.
(a)Wavelet energy.
(b)Trip signal.

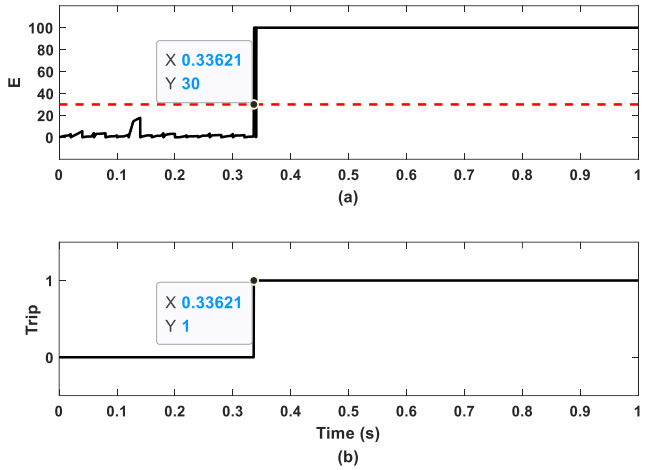

Fig. 9 Phase to phase to ground fault in looped microgrid.
(a)Wavelet energy.
(b)Trip signal.

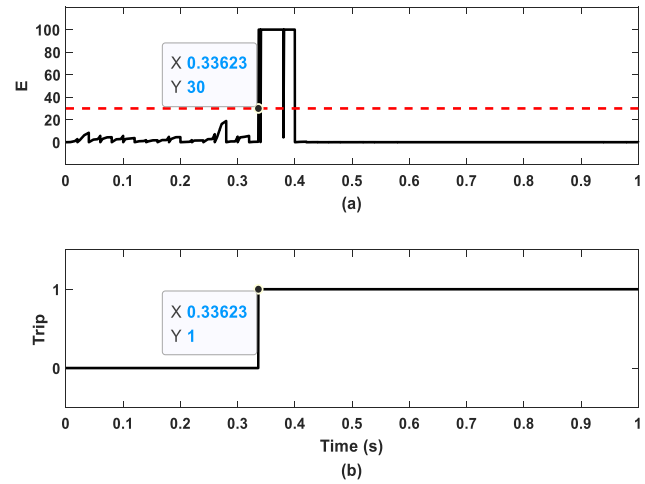

Fig. 10 Three phase to ground fault in radial microgrid.
(a) Wavelet energy.
(b) Trip signal.

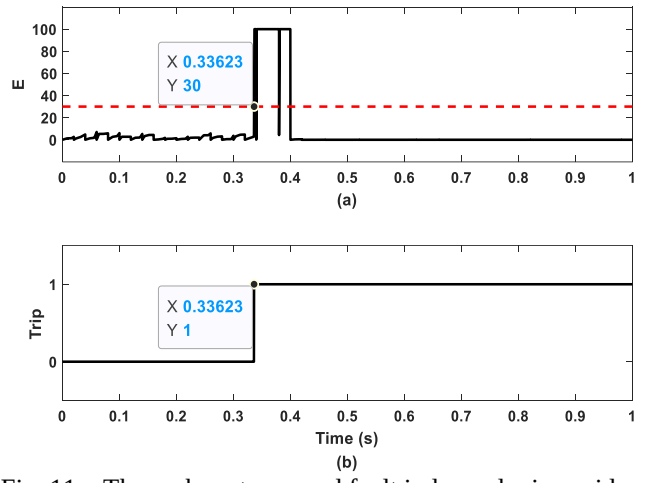

Fig. 11 Three phase to ground fault in looped microgrid.
(a) Wavelet energy.
(b) Trip signal.

5 Conclusion

In this paper, a voltage-based protection scheme is developed using the discrete wavelet transform. In this scheme, the energy of wavelet coefficient is computed to indicate the fault scenarios. This protection system is tested by using the different fault types with varied microgrid structures and fault impedances. Based on the results from these case studies, the faults can be detected less than 70 ms even in the high impedance fault condition, which is fast enough for the protection of low voltage microgrid. Additionally, the sampling frequency of the scheme can be easily achieved (1 kHz) and it is based on the local measurement only and there is no need for any communication media, therefore, the scheme can be implemented in cost effective way, and is much more attractive than other communication based schemes.

6 References

[1] B. Kroposki *et al*., "Achieving a 100% Renewable Grid: Operating Electric Power Systems with Extremely High Levels of Variable Renewable Energy," in *IEEE Power and Energy Magazine*, 2017, 15, (2), pp. 61-73

[2] J. Rocabert, A. Luna, F. Blaabjerg and P. Rodríguez, "Control of Power Converters in AC Microgrids," in *IEEE Transactions on Power Electronics*, 2012, 27, (11), pp. 4734-4749

[3] A. Uddin Khan, Q. Hong, A. Dyśko and C. Booth, "Review and Evaluation of Protection Issues and Solutions for Future Distribution Networks," *2019 54th International Universities Power Engineering Conference (UPEC)*, Bucharest, Romania, 2019, pp. 1-6

[4] P. T. Manditereza and R. C. Bansal, "Review of technical issues influencing the decoupling of DG converter design from the distribution system protection strategy," in IET Renewable Power Generation, 2018, 12, (10), pp. 1091-1100

[5] M. N. Alam, "Adaptive Protection Coordination Scheme Using Numerical Directional Overcurrent Relays," in *IEEE Transactions on Industrial Informatics*, 2019, 15, (1), pp. 64-73

[6] M. Y. Shih, A. Conde, Z. Leonowicz and L. Martirano, "An Adaptive Overcurrent Coordination Scheme to Improve Relay Sensitivity and Overcome Drawbacks due to Distributed Generation in Smart Grids," in IEEE Transactions on Industry Applications, 2017, 53 (6), pp. 5217-5228

[7] F. Coffele, C. Booth and A. Dyśko, "An Adaptive Overcurrent Protection Scheme for Distribution Networks," in IEEE Transactions on Power Delivery, 2015, 30 (2), pp. 561-568

[8] E. Sortomme, S. S. Venkata and J. Mitra, "Microgrid Protection Using Communication-Assisted Digital Relays," in *IEEE Transactions on Power Delivery*, 2010, 25, (4), pp. 2789-2796

[9] X. Li, A. Dyśko and G. Burt, "Enhanced protection for inverter dominated microgrid using transient fault information," *11th IET International Conference on Developments in Power Systems Protection (DPSP 2012)*, Birmingham, UK, 2012, pp. 1-5

[10] D. Liu, D. Tzelepis and A. Dyśko, "Protection of Microgrids With High Amounts of Renewables: Challenges and Solutions," *2019 54th International Universities Power Engineering Conference (UPEC)*, Bucharest, Romania, 2019, pp. 1-6

[11] H. Al-Nasseri, M. A. Redfern and F. Li, "A voltage based protection for micro-grids containing power electronic converters," *2006 IEEE Power Engineering Society General Meeting*, Montreal, Que., 2006, pp.1-7

[12] P. Kanakasabapathy and M. Mohan, "Digital protection scheme for microgrids using wavelet transform," *2015 IEEE International Conference on Electron Devices and Solid-State Circuits (EDSSC)*, Singapore, 2015, pp. 664-667

[13]W. Gao and J. Ning, "Wavelet-Based Disturbance Analysis for Power System Wide-Area Monitoring," in *IEEE Transactions on Smart Grid*, 2011, 2, (1), pp. 121-130

[14] S. Papathanassiou, H. Nikos, and S. Kai, “A benchmark low voltage microgrid network,” Proc. CIGRE Symp. power Syst. with dispersed Gener., 2005, pp. 1–8

[15] D. P. Mishra, S. R. Samantaray and G. Joos, "A Combined Wavelet and Data-Mining Based Intelligent Protection Scheme for Microgrid," in *IEEE Transactions on Smart Grid*, 2016, 7, (5), pp. 2295-2304

[16] A. E. Emanuel, D. Cyganski, J. A. Orr, S. Shiller and E. M. Gulachenski, "High impedance fault arcing on sandy soil in 15 kV distribution feeders: contributions to the evaluation of the low frequency spectrum," in *IEEE Transactions on Power Delivery*, 1990, 5, (2), pp. 676-686

[17] T. M. Lai, L. A. Snider, E. Lo and D. Sutanto, "High-impedance fault detection using discrete wavelet transform and frequency range and RMS conversion," in *IEEE Transactions on Power Delivery*, 2005, 20, (1), pp. 397-407

[18] V. C. Nikolaidis, A. D. Patsidis and A. M. Tsimtsios, "High impedance fault modelling and application of detection techniques with EMTP-RV," in *The Journal of Engineering*, 2018, 2018, (15), pp. 1120-1124